Integrated Flood, Transport, and Economic Exposure Assessment Using Sentinel-1 SAR: A Case Study of Cyclone Ditwah

1st H.S.R. Hettikankanama
Department of Decision Sciences, Faculty of Business
University of Moratuwa
Moratuwa, Sri Lanka
hettikankanamahsr.24@uom.lk

2nd S.M. Dassanayake
Department of Decision Sciences, Faculty of Business
University of Moratuwa
Moratuwa, Sri Lanka
sandund@uom.lk

3rd T.S. De Silva
Department of Decision Sciences, Faculty of Business
University of Moratuwa
Moratuwa, Sri Lanka
tilokad@uom.lk

4th I. Mahakalanda.
Department of Decision Sciences, Faculty of Business
University of Moratuwa
Moratuwa, Sri Lanka
indram@uom.lk

5th N.C.N.Kaluarachchi
Department of Decision Sciences, Faculty of Business
University of Moratuwa
Moratuwa, Sri Lanka
kaluarachchincn.25@uom.lk

6th N.S.Abeysiriwardhana
Department of Decision Sciences, Faculty of Business
University of Moratuwa
Moratuwa, Sri Lanka
abeysiriwardhanans.20@uom.lk

Abstract*—Flooding remains one of the most destructive natural hazards worldwide, causing substantial infrastructure damage, economic disruption, and social vulnerability, particularly in rapidly urbanising tropical regions. In November 2025, Cyclone Ditwah brought intense rainfall to western Sri Lanka, leading to widespread inundation in the Gampaha Divisional Secretariat Division. This study develops and evaluates an integrated geospatial framework combining flood detection, transport network disruption analysis, and economic exposure assessment using Sentinel-1 Synthetic Aperture Radar (SAR) data. Pre-flood (1–15 November 2025) and post-flood (28 November–4 December 2025) C-band SAR imagery were processed through radiometric calibration, speckle filtering, terrain correction, and logarithmic backscatter differencing to derive a binary flood mask. The inundation layer was subsequently integrated with a connectivity-classified road network and a geocoded economic establishment dataset to evaluate transport disruption and spatial-economic exposure using an Economic Activity Exposure Index (EAEI) and Local Moran's I clustering. The proposed workflow was evaluated using 540 stratified validation points derived from independent high-resolution reference data. Validation results yielded an overall accuracy of 81.5%, precision of 79.3%, recall of 85.2%, F1-score of 82.1%, and a Cohen's Kappa coefficient of 0.63, indicating substantial agreement and suitability for rapid post-flood assessment. Results reveal that flooding disproportionately affected highly connected transport corridors and economically clustered zones, suggesting localised but structurally significant disruption. The study demonstrates the operational usefulness of Sentinel-1 SAR for rapid flood assessment and highlights the importance of integrating hazard mapping with infrastructure topology and economic clustering to support geospatial decision-making for disaster risk management.

Keywords—Change Detection, Cyclone Ditwah, Decision Support Systems, Economic Exposure, Flood Mapping Disaster Management

I. Introduction

Floods remain one of the most frequent and economically damaging natural hazards worldwide [1]. Climate change has increased the frequency and intensity of extreme rainfall events, particularly in densely populated and rapidly urbanising regions [2]. South Asia is especially vulnerable due to monsoonal variability and cyclone systems originating from the Bay of Bengal [3]. In Sri Lanka, recurrent flooding is intensified by tropical rainfall, low-lying terrain, dense settlements, and modified drainage systems. The Gampaha Divisional Secretariat (DS) Division in western Sri Lanka represents a rapidly urbanising area with mixed residential, commercial, and agricultural land uses, where settlement concentration and transportation corridors increase vulnerability to localised flooding during extreme rainfall events.

In November 2025, Cyclone Ditwah caused intense rainfall and widespread flooding within the Gampaha DS Division, affecting settlements, infrastructure, agricultural lands, and transportation corridors. Such events increase pressure on emergency response systems and highlight the need for timely spatial information for evacuation planning and post-disaster assessment [5]. In data-scarce environments, satellite-based flood detection has become an important component of geospatial Decision Support Systems (DSS). Synthetic Aperture Radar (SAR) is particularly effective for flood monitoring because it penetrates cloud cover and operates independently of daylight conditions [6]. Sentinel-1 SAR imagery supports rapid inundation mapping through pre- and post-event backscatter change detection [7]–[9].

While flood extent mapping provides essential hazard intelligence, understanding disaster impacts requires examining functional disruption within urban systems. Transportation networks represent structurally central components that sustain mobility, economic exchange, and emergency access. Flood-induced disruption of highly connected road segments can disproportionately affect accessibility and urban cohesion. Therefore, beyond mapping inundation extent, it is necessary to evaluate how floodwaters intersect with topologically significant components of the transport network. Flood impacts must also be interpreted in terms of economic exposure. Urban economic systems are spatially clustered, and concentrations of commercial, service, and production establishments create localised zones of heightened vulnerability. Assessing the spatial distribution, sectoral composition, and clustering of economic activities

XXX-X-XXXX-XXXX-X/XX/$XX.00 ©20XX IEEE

https://doi.org/10.54389/NCFF8252

enables identification of areas where hydrological hazards coincide with economically significant concentrations. Integrating hazard mapping with transport connectivity and economic exposure analysis thus provides a systemic perspective on disaster impacts.

Within the Sri Lankan context, recent studies have emphasised the integration of geospatial intelligence into hazard resilience and disaster-management frameworks. Dassanayake et al. [10] highlighted the importance of spatially explicit hazard-risk modelling for disaster-informed planning, while Prasanna et al. [11] emphasised the role of spatial decision-support systems in strengthening disaster management strategies. However, limited research has focused on validated, event-specific SAR-based flood detection at divisional administrative scales while simultaneously integrating transport-network topology and economic exposure analysis. This study addresses that gap by developing and evaluating a Sentinel-1 SAR-based geospatial assessment workflow for the Cyclone Ditwah flood event in the Gampaha DS Division. Pre- and post-event Sentinel-1 imagery was used to implement a backscatter change-detection approach for inundation mapping. The derived flood mask was integrated with a connectivity-classified road network to identify structurally important transport segments exposed to flooding. Validation was conducted using independent high-resolution reference data through confusion-matrix-based metrics, including Overall Accuracy, Precision, Recall, F1-score, and Cohen's Kappa coefficient [16], [17]. Furthermore, spatial economic exposure was assessed using geocoded establishment data and clustering analysis, providing a practical DSS-ready framework for rapid post-flood assessment and disaster-risk management..

II. Literature Review

Flooding is one of the most destructive climate-related hazards globally, causing severe impacts on infrastructure, transportation systems, economic activity, and human settlements [1], [2]. Climate variability and rapid urban expansion have further increased flood vulnerability in densely populated tropical regions, where drainage limitations and land-use transformation intensify disaster impacts [1]. Traditional hydrological monitoring methods often face limitations during rapidly evolving flood events due to restricted spatial coverage and accessibility constraints [4]. Remote sensing technologies, particularly Synthetic Aperture Radar (SAR), have become widely used for rapid flood detection because they can acquire data independent of cloud cover and daylight conditions [5], [6]. Sentinel-1 SAR imagery has proven especially effective for operational flood mapping due to its frequent revisit cycle, open accessibility, and sensitivity to water-induced backscatter reduction [5], [7]. Multi-temporal SAR change-detection approaches have been successfully applied for inundation extraction using pre- and post-event backscatter comparison [6]. In urban environments, high-resolution SAR datasets such as TerraSAR-X have also demonstrated the capability to detect flooding under complex built-up conditions [9]. These studies confirm the operational value of SAR-based flood mapping for rapid disaster assessment and emergency response. Within the Sri Lankan context, previous studies have applied geospatial approaches for flood-risk assessment and multi-hazard vulnerability mapping [10], [11]. However, most studies mainly focus on flood extent or hazard susceptibility, with limited attention given to transport disruption and economic exposure caused by inundation. Recent reports related to Cyclone Ditwah further emphasise the need for rapid assessment tools capable of supporting emergency response and recovery planning in highly affected districts such as Gampaha [12], [13].

Recent studies have also highlighted the importance of integrating socio-economic and functional urban characteristics into spatial analysis. Point-of-Interest (POI)-based approaches have increasingly been used to evaluate economic concentration, mixed land use, and urban activity patterns [19]–[21]. Such datasets provide valuable insight into the spatial distribution of services and economic functions, supporting more operational disaster assessments. Disaster risk studies have further emphasised the need for integrated vulnerability and exposure analysis for effective decision-support systems [22]. Despite these advancements, a significant research gap remains in integrating validated SAR-based flood detection with transport-network disruption analysis and spatial-economic exposure assessment within a single operational workflow. Furthermore, few studies in Sri Lanka have combined Sentinel-1 flood mapping with connectivity-based transport analysis and POI-driven economic clustering for rapid post-disaster decision-making [23]. Therefore, this study develops and evaluates an integrated geospatial framework combining Sentinel-1 SAR flood detection, transport-network disruption analysis, and economic exposure assessment for the Cyclone Ditwah flood event in the Gampaha Divisional Secretariat Division.

III. Methodology

A. Study Area

The study focuses on the Gampaha Divisional Secretariat (DS) Division in western Sri Lanka, an area characterised by low elevation, dense settlements, rapid urban expansion, and interconnected drainage channels that increase flood vulnerability. In November 2025, Cyclone Ditwah caused widespread inundation, affecting settlements, transport networks, and economic activities across several GN divisions. The administrative boundary of the Gampaha DS Division was used as the spatial extent for analysis. The geographical location of the study area is illustrated in Fig. 1.

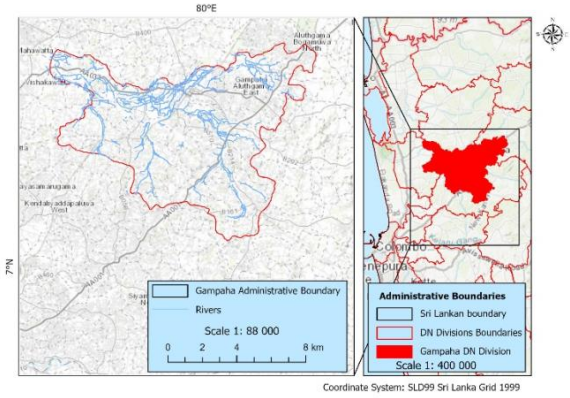

Fig.1. Study area map

B. Data and Methods

Fig. 2 shows the methodological framework adopted in this study.

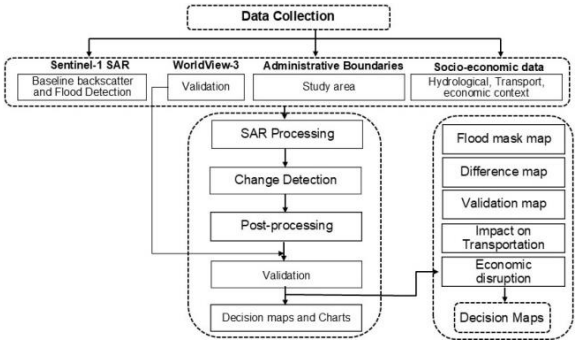

Fig.2. Methodological framework

The framework outlines the sequential process from data collection through SAR preprocessing, change detection, post-processing, validation, and generation of decision-support flood maps. The workflow integrates Sentinel-1 Synthetic Aperture Radar (SAR) imagery, WorldView 3 satellite data, administrative boundary layers, and river network information to generate and validate a flood mask following Cyclone Ditwah.

1) Data

This study integrates multi-source geospatial datasets for flood detection, transport disruption analysis, and economic exposure assessment following Cyclone Ditwah. Sentinel-1 Ground Range Detected (GRD) SAR imagery was obtained from the ESA Copernicus Open Access Hub, with pre-flood data acquired between 1–15 November 2025 and post-flood data between 28 November and 4 December 2025. The C-band SAR imagery, with approximately 10 m spatial resolution, was used for flood delineation under cloud-covered conditions. High-resolution UAV orthomosaic imagery from OpenAerialMap was manually digitised to generate reference flood polygons for validation. The Gampaha DS boundary, river network, and road data were derived from national datasets and OpenStreetMap (OSM). Economic establishments were compiled from public directories and OSM POI data, classified into seven sectors, and geocoded for spatial analysis. All datasets were projected to Sri Lanka Grid (SLD99) for consistency. The datasets, sources, acquisition periods, spatial resolutions, and analytical purposes are summarised in Table I.

TABLE I. ESSENTIAL DATASETS USED FOR FLOOD DETECTION AND VALIDATION

Data Type	Source	Date	Resolution	Purpose
Sentinel-1 SAR (Pre)	ESA Copernicus	1–15 Nov 2025	10 m	Baseline backscatter
Sentinel-1 SAR (Post)	ESA Copernicus	28 Nov–4 Dec 2025	10 m	Flood detection
Satellite data	OpenAerialMap	Dec 2025	~5–10 cm	Ground validation
Gampaha DS Boundary	Survey Dept. Sri Lanka	2023	-	Clipping extent
River Layer, Road Network, Economic data	Survey Dept. / OSM	2023	-	Hydrological, Transport, economic context

2) Methods

Sentinel-1 SAR GRD imagery was processed using standard radar preprocessing techniques to ensure radiometric and geometric consistency. The VV polarization channel was selected for change detection. Flood detection was performed using a multi-temporal backscatter difference approach. The backscatter difference image was calculated using Eq(1).

$$\Delta\sigma^0 = \sigma^{\sigma}_{\text{post-flood}} - \sigma^{\sigma}_{\text{pre-flood}} \qquad \text{Eq(1)}$$

where $\sigma^0_{\text{pre-flood}}$ represents the median pre-event VV backscatter and $\sigma^0_{\text{post-flood}}$ represents the median post-event VV backscatter. Negative backscatter differences were interpreted as potential inundation because smooth water surfaces reduce radar return. A threshold-based classification was then applied to extract the binary flood mask, followed by post-processing to remove isolated noise pixels and improve spatial consistency.

Orbit file correction was first applied to refine satellite positioning. Radiometric calibration was performed to convert digital numbers into sigma naught (σ^0) backscatter values. Speckle noise, inherent in SAR imagery due to coherent signal interference, was reduced using a Lee filter to improve classification stability. Terrain correction was applied using a Range-Doppler method to account for geometric distortions. The calibrated backscatter values were converted to decibel (dB) scale for analysis. Flood detection was implemented using a logarithmic subtraction approach (After - Before) to identify areas exhibiting significant reductions in backscatter indicative of open water surfaces. A threshold was empirically selected based on histogram analysis of the difference image to generate a binary flood mask. Post-processing steps included removal of isolated pixels, smoothing of classification boundaries, and clipping to the Gampaha DS administrative boundary. The primary outputs consisted of a flood mask and a backscatter difference map. Infrastructure-level impacts were evaluated by spatially intersecting the extracted flood mask with the road-network layer. The road dataset was converted into a graph-based network to compute connectivity metrics and classify segments according to functional importance. Flood-affected road lengths were calculated and summarised by connectivity class to identify potential disruption to accessibility and movement within the transport system. Economic exposure was assessed by aggregating geocoded establishments into a grid-based framework and calculating establishment density per cell. The values were normalised to derive the Economic Activity Exposure Index (EAEI) using Eq. (2), where higher values indicate stronger economic concentration. Spatial clustering patterns were identified using Local Moran's I

(LISA), while the Shannon Diversity Index was used to evaluate sectoral diversity within each grid cell. This integrated approach enabled assessment of both physical flood exposure and broader functional-economic disruption.

$$EAEI_i = x_i - x_{min}/x_{max} - x_{min} \quad \text{Eq(2)}$$

where $x_i$is the number of establishments in grid cell i, and $x_{\min}$ and $x_{\max}$ represent the minimum and maximum establishment counts across all grid cells. Values closer to 1 indicate stronger concentration of economic activity and therefore greater potential exposure if the cell overlaps with inundated areas.

3) Validation and Evaluation Design

Validation was conducted using independent high-resolution reference data obtained through OpenAerialMap/UAV-based visual interpretation. Flooded and non-flooded reference areas were digitised from the orthomosaic imagery, and 540 stratified random validation points were generated to ensure balanced representation of both classes and to minimise sampling bias. Each validation point was spatially overlaid with the classified flood mask and assigned to one of four confusion-matrix categories: true positive (TP), true negative (TN), false positive (FP), or false negative (FN). The validation process resulted in 230 TP, 210 TN, 60 FP, and 40 FN samples. Model performance was evaluated using Overall Accuracy (OA), Precision, Recall, F1-score, and Cohen's Kappa coefficient. Overall Accuracy measured total classification agreement, Precision evaluated the reliability of mapped flooded pixels, Recall assessed the ability of the model to identify actual flooded areas, and the F1-score provided a balanced measure of Precision and Recall. Cohen's Kappa was used to assess agreement beyond chance. The validation results yielded an Overall Accuracy of 81.5%, Precision of 79.3%, Recall of 85.2%, and an F1-score of 82.1%, while the Cohen's Kappa coefficient of 0.63 indicated substantial agreement between the classified flood mask and the reference data. These results demonstrate that the Sentinel-1 SAR change-detection framework provides reliable flood delineation suitable for rapid post-flood assessment and operational decision-support applications. In addition to flood-map accuracy assessment, the practical usefulness of the workflow was further evaluated through spatial exposure analysis. The validated flood mask was intersected with the connectivity-classified road network to identify potentially disrupted transport corridors, and overlaid with economic activity grids to examine areas where inundation coincided with concentrated economic establishments. This integrated evaluation framework enabled assessment not only of flood-detection accuracy, but also of the broader infrastructural and economic implications of flooding.

IV. Results

A. Flood Hazard Results

Sentinel-1 SAR change detection reveals clear spatial patterns of inundation within the Gampaha DS Division. Figure 3 presents the pre- and post-flood backscatter maps and the corresponding difference image (After – Before), where significant reductions in backscatter indicate newly inundated areas following Cyclone Ditwah

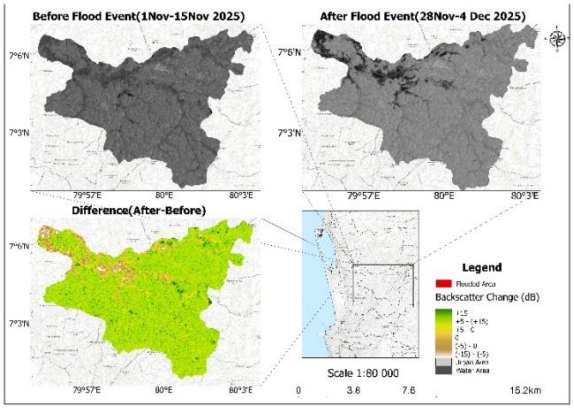

Fig. 3. Pre-flood (1–15 Nov 2025), post-flood (28 Nov-4 Dec 2025), and backscatter difference (After - Before) maps.

. These reductions reflect smooth water surfaces that attenuate radar returns. Figure 4 shows the final binary flood mask derived through thresholding and post-processing. Inundation is concentrated in low-lying terrain and areas adjacent to the river layer, demonstrating strong spatial consistency with hydrological features. The extracted flood extent serves as the primary analytical output and forms the basis for validation and subsequent decision-support assessments.

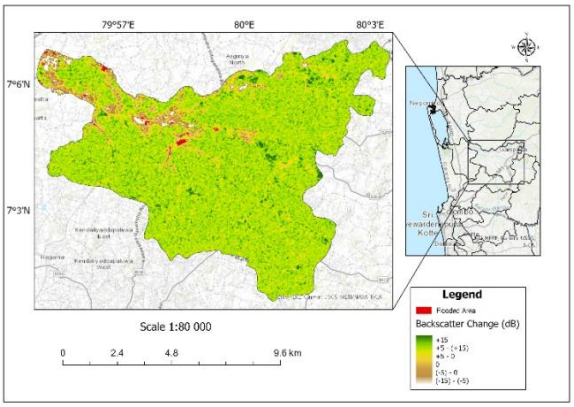

Fig. 4. Final flood mask map showing inundated areas

Quantitative validation was conducted using 540 randomly generated validation points compared against WorldView 3 satellite reference data. The confusion matrix was obtained through spatial overlay validation.

The model correctly identified 230 flooded points (True Positives, TP) and 210 non-flooded points (True Negatives, TN), while 60 points were classified as False Positives (FP) and 40 as False Negatives (FN). TABLE II. shows that the model achieved an Overall Accuracy (OA) of 81.5%, with a Kappa coefficient of 0.63, indicating substantial agreement between the SAR-derived flood mask and WorldView 3 satellite data. The Recall value (85.2%) indicates strong capability in detecting flooded pixels, while Precision (79.3%) suggests moderate overestimation in certain areas. The F1-score of 82.1%, which represents the harmonic mean of Precision and Recall, provides a balanced measure of classification

performance by accounting for both detection sensitivity and false alarm rates. The results confirm that Sentinel-1 SAR change detection can effectively delineate flood extents associated with Cyclone Ditwah in the Gampaha DSD.

TABLE II. ACCURACY METRICS DERIVED FROM CONFUSION MATRIX

Metric	Value
Overall Accuracy (OA)	81.5%
Precision	79.3%
Recall (Sensitivity)	85.2%
F1-Score	82.1%
Cohen's Kappa	0.63

The validation results indicate that the flood-detection model was more effective in identifying actual flooded areas than avoiding overclassification. A recall value of 85.2% shows that most inundated locations were successfully detected, while the precision value of 79.3% suggests moderate overclassification associated with wet soil, smooth surfaces, and low-backscatter conditions. Therefore, the flood mask is suitable for rapid operational assessment and planning support. SAR backscatter analysis identified concentrated flooding in western and central GN divisions, including Bollatha North, Midellavita, Kudabollatha, and Rathmalvita. These areas also show higher economic vulnerability, indicating localised clusters of compounded flood and socio-economic risk requiring targeted mitigation measures..

B. Transport Disruption

Fig. 5 illustrates the intersection between the flood mask and the connectivity-classified road network. Flooding primarily affects highly connected road segments, particularly in the central and north-western zones where transport corridors support dense settlements and commercial activity. This indicates that impacts extend beyond physical road submergence to functional disruption of spatial connectivity. The findings suggest that Cyclone Ditwah caused localised but structurally significant transport interruptions within the Gampaha Division.

Road connectivity class	Total road length	Flood-affected road length	Percentage affected
High	239.06 km	0.74 km	0.31%
Medium	345.75 km	2.65 km	0.77%
Low	417.46 km	6.40 km	1.53%
Total	1002.27 km	9.79 km	0.98%

The results indicate whether flood impacts were concentrated on structurally important road segments or mainly distributed across peripheral links. Higher exposure of connected roads suggests greater functional disruption to accessibility, emergency movement, and local mobility. This analysis extends the workflow beyond flood mapping toward practical transport-disruption assessment.

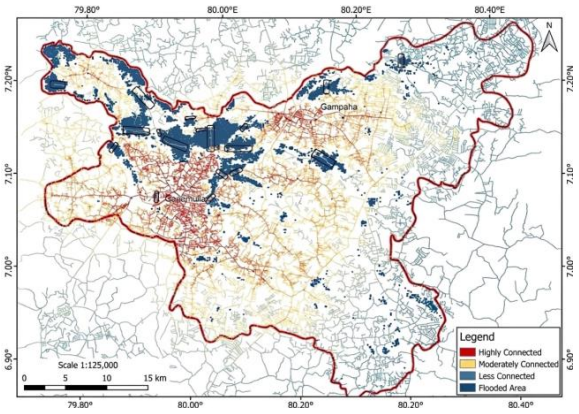

Fig. 5. Flood impact on the road network

C. Economic Activity Exposure Patterns

TABLE III. summarises the economic exposure characteristics of the Gampaha DS Division. A total of 534 establishments were mapped across seven sector classes. The mean EAEL is 0.3, indicating moderate normalised exposure, while the mean Shannon Index of 1.9 (close to the theoretical maximum ln (7) ≈ 1.95) reflects high sectoral diversification. The Global Moran's I value of 0.1768 (p = 0.001) confirms significant positive spatial autocorrelation, indicating clustered patterns of economic exposure rather than random distribution.

TABLE III. SUMMARY STATISTICS OF ECONOMIC EXPOSURE CHARACTERISTICS

Metric	Value
Total mapped economic establishments	534
Number of sector classes	7
Mean EAEI	0.3
Mean sector diversity	1.9
Global Moran's I	0.1768
p-value	0.001

V. DISCUSSION

The results demonstrate that the proposed workflow is practically applicable for rapid post-flood assessment. The Sentinel-1 SAR-based flood detection achieved an overall accuracy of 81.5% and a Cohen's Kappa of 0.63, indicating substantial agreement with independent reference data. The relatively high recall value suggests that the method is effective in detecting most inundated areas, which is important for emergency response and preliminary damage assessment. The precision value indicates that some overestimation occurred. This is a common limitation in SAR-based flood mapping, particularly in urban and mixed land-cover environments where wet soil, smooth surfaces, and radar shadow may produce low-backscatter responses similar to open water. Therefore, the flood mask should be interpreted as a rapid assessment product rather than a final cadastral-scale flood boundary. The transport-disruption analysis adds practical value by showing how flood exposure intersects with the functional structure of the road network. Flooding of highly connected road segments can have wider

consequences for accessibility, emergency response, and local mobility than flooding of isolated roads. This demonstrates why integrating flood masks with road-network characteristics is important for disaster management. The economic exposure analysis further extends the usefulness of the flood map by identifying areas where inundation overlaps with concentrated economic activity. This is important because flood impacts are not determined only by water extent, but also by the social and economic functions located within affected areas. The integration of EAEI and LISA-based clustering helps identify priority areas for recovery planning and resource allocation. Several limitations should be acknowledged. First, SAR-based flood detection may overestimate inundation in areas with wet bare soil, radar shadow, smooth paved surfaces, or low-backscatter land-cover conditions. Second, the 10 m spatial resolution of Sentinel-1 may limit the detection of narrow drainage channels and small urban flood patches. Third, the road-disruption analysis is based on spatial intersection and network connectivity rather than observed traffic-flow data. Fourth, the economic exposure analysis is based on available geocoded establishments and may underrepresent informal or unregistered businesses. Therefore, the outputs should be interpreted as rapid decision-support indicators rather than exact estimates of total economic loss or transport delay.

VI. Conclusion

This study developed and evaluated an integrated geospatial workflow for assessing flood extent, transport exposure, and economic activity exposure following Cyclone Ditwah in the Gampaha DS Division. The Sentinel-1 SAR flood-detection component achieved an overall accuracy of 81.5%, recall of 85.2%, F1-score of 82.1%, and Cohen's Kappa of 0.63, demonstrating its suitability for rapid post-flood assessment. By linking the flood mask with road-network connectivity and economic activity concentration, the study moves beyond hazard mapping and provides decision-support information on areas where flooding may generate wider functional and economic disruption. The workflow is particularly useful for data-constrained urban environments where rapid, spatially explicit post-disaster assessment is required.

Acknowledgement

The authors gratefully acknowledge the financial support provided by the University of Moratuwa through the SRC Grant (Grant No. SRC/LT/2024/06). The authors also extend their sincere appreciation to Ravindu Thamodya for assistance in collecting socio-economic data, and to the academic and technical staff who supported throughout the study.

References

[1] IPCC, Climate Change 2023: Impacts, Adaptation and Vulnerability. Cambridge, U.K.: Cambridge Univ. Press, 2023.

[2] United Nations Office for Disaster Risk Reduction (UNDRR), Global Assessment Report on Disaster Risk Reduction 2022, Geneva, Switzerland, 2022.

[3] A. K. Mishra and V. P. Singh, "A review of drought concepts," Journal of Hydrology, vol. 391, no. 1–2, pp. 202–216, 2010.

[4] H. Brakenridge, S. V. Nghiem, E. Anderson, and R. Mic, "Orbital remote sensing of river discharge and ice status," Water Resources Research, vol. 41, no. 4, 2005.

[5] C. Ticehurst, R. D. Jones, and J. M. Chen, "Operational flood mapping using Sentinel-1 SAR data," Remote Sensing, vol. 11, no. 10, pp. 1–19, 2019.

[6] M. Pulvirenti, M. Chini, N. Pierdicca, L. Guerriero, and P. Ferrazzoli, "Flood monitoring using multi-temporal COSMO-SkyMed data," IEEE Journal of Selected Topics in Applied Earth Observations and Remote Sensing, vol. 4, no. 2, pp. 350–362, 2011.

[7] European Space Agency (ESA), "Sentinel-1 User Guide," ESA, Paris, France, 2023. [Online]. Available: https://sentinel.esa.int

[8] European Space Agency (ESA), "Sentinel-2 User Guide," ESA, Paris, France, 2023. [Online]. Available: https://sentinel.esa.int

[9] D. C. Mason, I. J. Davenport, R. J. Schumann, J. C. Neal, and P. D. Bates, "Flood detection in urban areas using TerraSAR-X," IEEE Transactions on Geoscience and Remote Sensing, vol. 50, no. 8, pp. 3044–3058, 2012.

[10] P. Prasanna, S. Dassanayake, and R. Jayasinghe, "Geospatial analytics for flood risk assessment in Sri Lanka," in Proc. International Conf. on Disaster Risk Reduction, Colombo, Sri Lanka, 2020, pp. 45–52.

[11] S. Dassanayake and P. Prasanna, "Multi-hazard geospatial modelling for flood vulnerability mapping in Sri Lanka," International Journal of Disaster Risk Reduction, vol. 58, 2021.

[12] Disaster Management Centre (DMC), Sri Lanka, Situation Report: Cyclone Ditwa Flood Impact Assessment, Colombo, Sri Lanka, 2025.

[13] Department of Meteorology, Sri Lanka, Cyclone Ditwa Technical Report, Colombo, Sri Lanka, 2025.

[14] Department of Census and Statistics, Sri Lanka, Administrative Boundaries Dataset, Colombo, Sri Lanka, 2023.

[15] Google Earth Engine, "Sentinel-1 GRD dataset documentation," 2023. [Online]. Available: https://developers.google.com/earth-engine

[16] J. Cohen, "A coefficient of agreement for nominal scales," Educational and Psychological Measurement, vol. 20, no. 1, pp. 37–46, 1960.

[17] J. D. Congalton and K. Green, Assessing the Accuracy of Remotely Sensed Data: Principles and Practices, 2nd ed. Boca Raton, FL, USA: CRC Press, 2009.

[18] OpenAerialMap, "Gampaha flood UAV imagery dataset," 2025. [Online]. Available: https://map.openaerialmap.org/#/79.8046875,6.670063575977283

[19] Austin, P. A., Marini, M., Sanchez, A., Simpson-Bell, C., & Tebrake, J. (2021). Using the Google Places API and Google Trends Data to Develop High Frequency Indicators of Economic Activity. IMF Working Paper 2021/295.

[20] Psyllidis, A., Gao, S., Hu, Y., Kim, E.-K., McKenzie, G., Purves, R., Yuan, M., & Andris, C. (2022). Points of Interest (POI): a commentary on the state of the art, challenges, and prospects for the future. Computational Urban Science, 2, 20.

[21] Yue, Y., Zhuang, Y., Yeh, A. G. O., Xie, J.-Y., Ma, C.-L., & Li, Q.-Q. (2017). Measurements of POI-based mixed use and their relationships with neighbourhood vibrancy. International Journal of Geographical Information Science, 31(4), 658–675.

[22] Renteria-Ramos, R., Martinez-Cuevas, S., Vikaliana, R., & others. (2021). An entropy-based approach for disaster risk assessment and vulnerability management. Journal of Humanitarian Logistics and Supply Chain Management, 11(3), 428–453.